Published for SISSA by Springer

Received: *July 15, 2024*
Revised: *September 27, 2024*
Accepted: *October 8, 2024*
Published: *November 12, 2024*

New integrable RG flows with parafermions

Changrim Ahn[a,b] **and Zoltan Bajnok**[c]

[a] *Department of Physics, Ewha Womans University, Seoul 120-750, South Korea*
[b] *Institut für Physik, Humboldt-Universität zu Berlin, Zum Großen Windkanal 2, 12489 Berlin, Germany*
[c] *HUN-REN Wigner Research Centre for Physics, Konkoly-Thege Miklos ut 29-33, 1121 Budapest, Hungary*

E-mail: ahn@ewha.ac.kr, bajnok.zoltan@wigner.hu

Abstract: We consider irrelevant deformations of massless RSOS scattering theories by an infinite number of higher $[T\bar{T}]_s$ operators which introduce extra non-trivial CDD factors between left-movers and right-movers. It is shown that the resulting theories can be UV complete after bypassing typical Hagedorn-like singularities if the coefficients of the deformations are fine-tuned. By classifying all integrable cases, we have discovered a new UV complete QFT associated to the $\mathcal{M}_p$ ($p \geq 3$) minimal CFT based on the integrable structure of the RSOS scattering theory. This new theory is the massless $\mathbb{Z}_{p-1}$ parafermionic sinh-Gordon (PShG) model with a self-dual coupling constant. This correspondence is confirmed by showing that the scale-dependent vacuum energies computed by the thermodynamic Bethe ansatz derived from the S-matrices match those from the quantization conditions for the PShG models using the reflection amplitudes.

Keywords: Integrable Field Theories, Renormalization Group, Bethe Ansatz, Field Theories in Lower Dimensions

ArXiv ePrint: 2407.06582

Open Access, © The Authors.
Article funded by SCOAP[3].

https://doi.org/10.1007/JHEP11(2024)078

JHEP11(2024)078

Contents

1 Introduction **1**

2 Massless kink S-matrices and their TBA **2**
2.1 Restricted sine-Gordon model and massive kinks 2
2.2 Massless kinks scattering 4

3 $[T\bar{T}]$ deformations of RSOS S-matrices **7**
3.1 CDD factors 7
3.2 TBA and UV complete theories 8

4 Parafermionic sinh-Gordon model **10**
4.1 The sinh-Gordon model 10
4.2 The SShG model 11
4.3 Parafermionic Sinh-Gordon models 13

5 Comparing the TBA to the reflection amplitudes **14**
5.1 Effective central charge from the reflection amplitudes 14
5.2 Numerical solution of the TBA 16

6 Roaming TBA **17**

7 Conclusion **19**

A Magnonic scatterings with a CDD factor **20**
A.1 Massive scattering 20
A.2 Massless scattering and its irrelevant perturbations 22
A.3 Minimal models perturbed with $\Phi_{1,3}$ 24

1 Introduction

Integrable quantum field theories (QFTs) have special properties that can provide quantitative methods to study QFTs non-perturbatively [1]. Physically important cases are those QFTs whose renormalization group (RG) flows interpolate between the UV (ultra-violet) and IR (infra-red) conformal field theories (CFTs) [2]. In general, this class of QFTs is very difficult to study analytically since they become non-perturbative at the IR scale. Fortunately, integrable QFTs in two dimensions have provided quantitative methods to address this difficulty. A fundamental quantity in integrable QFTs is the exact scattering (S)-matrix between asymptotic particle states, which are determined by the IR physics such as on-shell symmetries and other axioms. From these exact S-matrices, thermodynamic Bethe ansatz (TBA) equations can be derived, whose solutions provide scaling functions which describe the RG flows at all scales [3].

JHEP11(2024)078

A traditional approach is to start with an UV CFT perturbed by a relevant operator which maintains integrability and to find the corresponding IR CFT with its S-matrix and identify its irrelevant deformations. Many exact S-matrices have been constructed in this way. In practice, exact RG flows have been found from the TBAs, some of which are not directly related to S-matrices [4–7, 9, 10]. Another interesting feature arises from the fact that different integrable QFTs may arise from a given UV CFT by different relevant perturbations. Hence, it is conceivable that several different UV CFTs may lead to a common IR CFT along their RG flows.

This possibility raises an important question, "Can we completely classify UV CFTs that can be reached from a given IR CFT?". To answer this question, we need a new approach of classifying all possible irrelevant operators of a given IR CFT. This problem has been studied recently in [11] by exploiting a special class of irrelevant operators belonging to the energy-momentum tensors and their descendants which preserve integrability [12, 13]. Constrained to diagonal scattering theories, it has been found that several UV CFTs can be reached from certain minimal IR CFTs. For example, there are about 4 UV CFTs which all flow into the critical Ising CFT. Some of these are new which have not been known in the earlier literature.

In this paper, we focus on non-diagonal scattering theories for which this approach can be more restrictive and powerful. In particular, we can identify all the UV CFTs and their relevant perturbations, and discover their explicit integrable QFTs which show new integrable flows into the *unitary minimal CFTs* in the IR limit.

This paper is organized as follows. In section 2, we review RSOS scattering theories and associated TBA systems. Their derivations are reviewed in appendix A. In section 3, we construct exact S-matrices and derive the TBA systems for the $[T\bar{T}]_s$-deformed unitary minimal models. We introduce in section 4 the Lagrangians and other exact known results of the PShG models and their UV CFTs, the parafermionic Liouville theories. In section 5, we identify these explicit QFTs with the deformed models by showing that the scaling function from the TBAs match with the results from the reflection amplitudes of the parafermionic theories. One byproduct of our approach is to discover new S-matrices which provide previously known roaming TBAs. This is explained in section 6. We will conclude the paper in section 7. The derivation of how a CDD factor modifies the TBAs for non-diagonal scattering theories is quite technical and we provide details in appendix A.

2 Massless kink S-matrices and their TBA

2.1 Restricted sine-Gordon model and massive kinks

We start with a minimal CFT $\mathcal{M}_p$ with a central charge $c = 1 - 6/(p(p+1))$ perturbed by the least relevant operator Φ_{pert} with a conformal dimension $h = (p-1)/(p+1)$, whose formal action can be written as

$$\mathcal{S}_\lambda = \mathcal{S}_{\mathcal{M}_p} + \lambda \int d^2x \; \Phi_{\text{pert}}. \tag{2.1}$$

This model is a well-known integrable QFT [1], which is related to the quantum sine-Gordon model with $\mathcal{U}_{\mathsf{q}}(\mathfrak{su}_2)$ quantum group symmetry, where the deformation parameter q is related to p [14]. The S-matrix of (2.1) for a given p is obtained by truncating the multi-soliton

JHEP11(2024)078

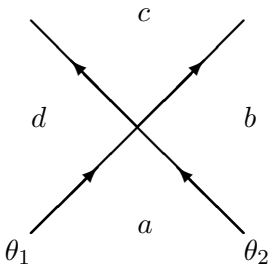


Figure 1. Kink S-matrix.

and antisoliton Hilbert space for q a root of unity. On-shell particles are "kinks" connecting two adjacent vacua denoted by the corresponding spins

$$a \;\Big\uparrow\; b \;=\; K_{ab}(\theta), \qquad a,b = 0,\frac{1}{2},\cdots,\frac{p}{2}-1, \quad \text{with} \quad |a-b|=\frac{1}{2}. \tag{2.2}$$

When $\lambda < 0$, the kink particles are massive with an energy and momentum

$$E = M\cosh\theta, \qquad P = M\sinh\theta, \tag{2.3}$$

where the mass M is related to λ by [17]

$$\pi|\lambda| = \frac{(p+1)^2}{(p-1)(2p-1)}\left[\frac{\gamma\left(\frac{3p}{p+1}\right)}{\gamma\left(\frac{1}{p+1}\right)}\right]^{1/2}\left[\frac{\sqrt{\pi}M\Gamma\left(\frac{p+1}{2}\right)}{2\Gamma\left(\frac{p}{2}\right)}\right]^{4/(p+1)}. \tag{2.4}$$

Here $\gamma(x) = \Gamma(x)/\Gamma(1-x)$. Amplitudes for two kinks scattering process in figure 1

$$K_{da}(\theta_1) + K_{ab}(\theta_2) \to K_{dc}(\theta_2) + K_{cb}(\theta_1) \tag{2.5}$$

are given by[1]

$$S_p(\theta)^{ab}_{dc} = U(\theta)\;(X^{ac}_{db})^{\frac{i\theta}{2\pi}}\left[(X^{ac}_{db})^{\frac{1}{2}}\sinh\left(\frac{\theta}{p}\right)\delta_{db} + \sinh\left(\frac{i\pi-\theta}{p}\right)\delta_{ac}\right], \tag{2.6}$$

where $U(\theta)$ is a well-known scalar factor of the sine-Gordon model ($\theta = \theta_1 - \theta_2$) given by

$$U(\theta) = \frac{1}{\sinh\frac{1}{p}(\theta - i\pi)}\exp\left[\int_{-\infty}^{\infty}\frac{dk}{k}\,\frac{\sinh\frac{k\pi(p-1)}{2}}{2\sinh\frac{k\pi p}{2}\cosh\frac{k\pi}{2}}e^{ik\theta}\right], \tag{2.7}$$

and

$$X^{ac}_{db} = \frac{[2a+1][2c+1]}{[2d+1][2b+1]} \tag{2.8}$$

with the q-number defined by

$$[n] = \frac{\mathsf{q}^n - \mathsf{q}^{-n}}{\mathsf{q}-\mathsf{q}^{-1}}, \qquad \text{with} \quad \mathsf{q} = -\exp\left(\frac{-i\pi}{p}\right). \tag{2.9}$$

[1] In a recent paper [15], a generalized crossing symmetry related to a non-invertible symmetry allows new S-matrix without the prefactor $(X^{ac}_{db})^{\frac{i\theta}{2\pi}}$. This gauge factor does not change the TBA.

JHEP11(2024)078

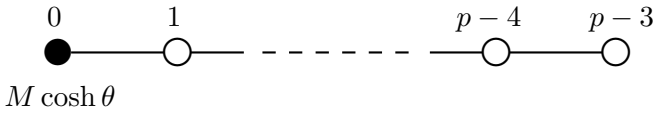


Figure 2. A_{p-2} Dynkin diagram for massive RSOS theories.

The exact two-particle S-matrices are obtained by a quantum group reduction of the scatterings of the quantum sine-Gordon model when the multi-soliton and antisoliton Hilbert space is truncated for the quantum group deformation parameter q a root of unity.

A fundamental tool to investigate scaling functions such as the vacuum energy for a given scale is TBA, which minimizes the free energy that is expressed by densities of on-shell particle states subject to periodic boundary condition (PBC) [3]. For non-diagonal scattering theories such as for the RSOS scattering theory above, deriving the TBA involves the difficult step of diagonalizing an inhomogeneous transfer matrix. This problem has been well studied both in QFTs and statistical lattice models in two dimensions. The eigenvalues are expressed in terms of new degrees of freedom, the so called "magnons" of $p-3$ different species, as well as the "physical" on-shell particles

$$\mathbb{T}_{\text{RSOS}}(\{\theta_i\})|\Psi\rangle = \Lambda\left(\{\theta_i\}, \oplus_{a=1}^{p-3}\{\alpha_j^{(a)}\}\right)|\Psi\rangle. \tag{2.10}$$

The TBA equations are obtained for the pseudo-energies corresponding to the densities of magnons and particles,

$$\epsilon_a(\theta) = \delta_{a0} MR\cosh\theta - \sum_{b=0}^{p-3} \mathbb{I}_{ab}\varphi \star \ln\left(1+e^{-\epsilon_b}\right)(\theta), \quad a = 0, \cdots, p-3, \tag{2.11}$$

where the "universal" kernel φ is given by

$$\varphi(\theta) = \frac{1}{\cosh\theta}, \tag{2.12}$$

$\star$ is the convolution and $\mathbb{I}$ is the adjacency matrix of the A_{p-2} Dynkin diagram, namely $\mathbb{I}_{ab}$ is 1 if nodes a and b are connected in figure 2 and zero otherwise.

2.2 Massless kinks scattering

We can think of the original conformal field theory as the $\lambda \to 0^-$ limit of the massive scattering theory. In this limit the scattering states become massless with a dispersion relation $E^2 = P^2$ between the energy (E) and momentum (P) carried by the asymptotic particles. The $E = +P$ and $E = -P$ cases describe right-moving (R) and left-moving (L) massless states, respectively. These states can be thought of as an extremely relativistic limit of massive states by rescaling all rapidities $\theta_i \to \hat{\theta}_i + \Lambda$ for (R) and $\theta_i \to \hat{\theta}_i - \Lambda$ for (L) in (2.3) and taking limits $M \to 0$, $\Lambda \to \infty$ while keeping $Me^{\Lambda} = \widehat{M}$ finite. We will take $\hat{\theta}$ as the rapidity from now on with which the dispersion relation is expressed as

$$E = \pm P = \frac{\widehat{M}}{2} e^{\pm\hat{\theta}}, \qquad + = R, \quad - = L. \tag{2.13}$$

JHEP11(2024)078

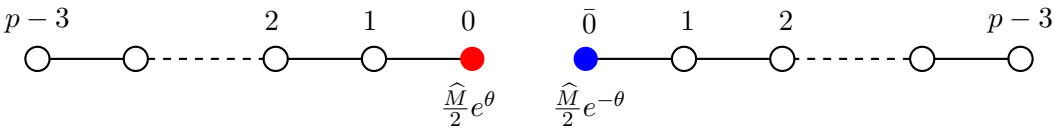


Figure 3. A_{p-2} Dynkin diagram for conformal RSOS theories.

In this limit, S-matrices between the same types (R or L) of massless particles are the same as the massive ones (2.6) because $\theta_1 - \theta_2 = \hat{\theta}_1 - \hat{\theta}_2$

$$S_p^{RR}(\theta) = S_p^{LL}(\theta) = S_p(\theta). \tag{2.14}$$

Scatterings between R and L particles become independent of the rapidities because $|\theta_1 - \theta_2| \to \infty$ and the kernels between these particles vanish in the TBA. Therefore, the TBA equations for massless kink theories are described by two separate sets (R and L) of equations,[2]

$$\epsilon_a^{\pm}(\theta) = \delta_{a0}\frac{\widehat{M}R}{2}e^{\pm\theta} - \sum_{b=0}^{p-3}\mathbb{I}_{ab}\varphi \star \ln\left(1 + e^{-\epsilon_b^{\pm}}\right)(\theta), \quad a = 0, \cdots, p-3, \tag{2.15}$$

where the adjacency matrix $\mathbb{I}_{ab}$ is given by figure 3. This TBA system describes the scale-invariant minimal CFT $\mathcal{M}_p$ since any change of the scale R can be absorbed into a shift of the rapidity θ.

Eq. (2.1) with $\lambda > 0$ was shown to generate an RG flow from a UV $\mathcal{M}_p$ CFT to the $\mathcal{M}_{p-1}$ IR CFT [2]. We can also think of the same flow the opposite direction, i.e. connecting the IR $\mathcal{M}_{p-1}$ minimal model to the UV $\mathcal{M}_p$ minimal model. As we already formulated the integrable scattering description of the $\mathcal{M}_p$ minimal model, we will concentrate on the (shifted) flow when the IR CFT is the $\mathcal{M}_p$ minimal model and the UV CFT is the $\mathcal{M}_{p+1}$ minimal model. This is a conceptual change of point of view. We would like to describe the flow by deforming the IR CFT with irrelevant operators. In the scattering language it means to introduce non-trivial scatterings between the left and right moving particles. The quantitative evaluation of the corresponding scaling function, such as the effective central charge, can be obtained by the TBA system first conjectured in [4].

This conjecture was confirmed based on the massless scattering theory in [7]. In this work, the $S_{\text{RSOS}}^{(p)RL}(\theta)$ scatterings between the left- and right-moving kinks were determined by the crossing-unitarity relations and the Yang-Baxter equation (YBE) between this and the $S_{\text{RSOS}}^{(p)RR}$, $S_{\text{RSOS}}^{(p)LL}$ scattering matrices giving

$$S_p^{RL}(\theta) = \frac{\tilde{U}(\theta)}{U(\theta + \frac{ip\pi}{2})}S_p\left(\theta + \frac{ip\pi}{2}\right), \quad S_p^{LR}(\theta) = -\frac{\tilde{U}(\theta)}{U(\theta - \frac{ip\pi}{2})}S_p\left(\theta - \frac{ip\pi}{2}\right), \tag{2.16}$$

where $\tilde{U}(\theta)$ is given by [7]

$$\tilde{U}(\theta) = \frac{1}{\cosh\frac{1}{p}(\theta - i\pi)}\exp\left[-\int_{-\infty}^{\infty}\frac{dk}{k}\frac{\sinh\frac{k\pi}{2}}{2\sinh\frac{k\pi p}{2}\cosh\frac{k\pi}{2}}e^{ik\theta}\right]. \tag{2.17}$$

[2]We will replace $\hat{\theta}$ with θ for the rapidity from now on and use superindex '+' for R-type and '−' for L-type in the TBA equations.

JHEP11(2024)078



Figure 4. A_{p-1} Dynkin diagram for massless RSOS theories.

The non-trivial scatterings between left and right movers modify the finite volume spectrum. As the RSOS part of the left-right scattering is shifted we have to diagonalize an inhomogenous transfer matrix, in which the inhomogeneities corresponding to the right movers are shifted. This shift implies that the right movers couple to the $p-3$ magnons differently: we have to flip that part of the Dynkin diagram. This was shown for $p=4$ rigorously and argued that the same happens with higher p's in [7] . In the appendix we present a mechanism how such a flip can happen for general p. This leads to the conjectured TBA in [2], whose adjacency matrix $\mathbb{I}_{ab}$ is given by the Dynkin diagram in figure 4,

$$\epsilon_a(\theta) = \delta_{a0}\frac{\widehat{M}R}{2}e^{\theta} + \delta_{a,p-2}\frac{\widehat{M}R}{2}e^{-\theta} - \sum_{b=0}^{p-2}\mathbb{I}_{ab}\varphi \star \ln\left(1+e^{-\epsilon_b}\right)(\theta), \quad a=0,\cdots,p-2, \tag{2.18}$$

where the two distinguished $R-$ and $L-$ nodes are colored red and blue, respectively. The ground-state energy at the scale R and effective central charge are defined by

$$E_0(R) = -\frac{\widehat{M}}{4\pi}\int_{-\infty}^{\infty}\left[e^{\theta}\ln\left(1+e^{-\epsilon_0(\theta)}\right)+e^{-\theta}\ln\left(1+e^{-\epsilon_{p-2}(\theta)}\right)\right]d\theta = -\frac{\pi C_{\text{eff}}(\widehat{M}R)}{6R}. \tag{2.19}$$

This TBA system generates a RG flow from the $\mathcal{M}_{p+1}$ CFT ($R=0$) to the $\mathcal{M}_p$ CFT ($R=\infty$).

Therefore, this set of S-matrices $S_p^{RR}(\theta), S_p^{LL}(\theta), S_p^{RL}(\theta), S_p^{LR}(\theta)$ describes the CFT $\mathcal{M}_p$ deformed by an irrelevant operator $\Phi_{3,1}$ and its descendants. The TBA given in (2.18) interpolates through an RG flow from the IR CFT $\mathcal{M}_p$ to the UV CFT $\mathcal{M}_{p+1}$.

Certainly, different irrelevant deformations will generate different flows to other UV CFTs perturbed by some relevant operators. For example, one simple possibility is to choose

$$S_p^{RR}(\theta) = S_p^{LL}(\theta) = S_p^{RL}(\theta) = S_p^{LR}(-\theta) = S_p(\theta). \tag{2.20}$$

This RL S-matrices do not have shifts in the rapidity shown in (2.16). In this case, a R-particle will scatter with both R- and L-particles with the same S-matrix in the virtual process when we move it around the periodic volume. The resulting PBC equation is obtained by the same transfer matrix as (2.10). In the same way, a L-particle will generate the same transfer matrix after scattering with all other particles. This common transfer matrix can be diagonalized and its eigenvalue is expressed in terms of the magnons. The resulting TBA equations are still given by (2.18) but with a different adjacency matrix in figure 5 where both R- and L-nodes are connected to the first magnon node. See the appendix how it happens in details. In fact this TBA has been already conjectured for a Parafermion CFT perturbed by a relevant bilinear parafermionic fields in [8] without specifying the S-matrices. The massless S-matrices in (2.20) provide them. The two cases above show clearly how the same LL and RR but different RL S-matrices based on the same IR CFT can describe different QFTs that reach at distinct UV CFTs.

JHEP11(2024)078

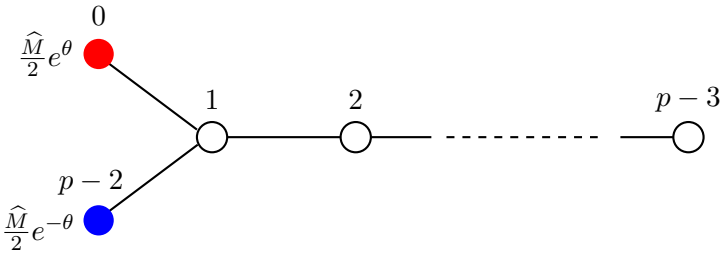


Figure 5. D_{p-1} Dynkin diagram for massless RSOS theories.

3 $[T\bar{T}]$ deformations of RSOS S-matrices

In this section, we deform an integrable QFT with a special set of irrelevant operators that maintain integrability with a deformed S-matrix. When a CFT is perturbed by a relevant operator Φ_{pert}, the holomorphic and anti-holomorphic conserved charges rearrange to satisfy new conserved local currents satisfying the continuity equations

$$\partial_{\bar{z}} T_{s+1} = \partial_z \Theta_{s-1}, \qquad \partial_z \bar{T}_{s+1} = \partial_{\bar{z}} \bar{\Theta}_{s-1}, \tag{3.1}$$

where s is a positive integer with $s+1$ and $-(s+1)$ the spins of T_{s+1} and $\bar{T}_{s+1}$ respectively. For $s=1$ these are the components of the universal stress-energy tensor and the conserved charges are the left and right components of the energy and momentum. For higher s, the above currents depend on the model, in particular the choice of Φ_{pert}. Smirnov and Zamolodchikov showed that from these one can construct well-defined local operators $[T\bar{T}]_s$:

$$[T\bar{T}]_s = T_{s+1}\bar{T}_{s+1} - \Theta_{s-1}\bar{\Theta}_{s-1} \tag{3.2}$$

with scaling dimension $(\text{mass})^{2(s+1)}$. More importantly, perturbation by such operators preserves integrability [12]. Thus, we can consider the theory defined by the action

$$\mathcal{S}_\lambda = \mathcal{S}_{\mathcal{M}_p} + \lambda \int d^2x\ \Phi_{3,1} + \sum_{s\geq 1} \alpha_s \int d^2x\, [T\bar{T}]_s \tag{3.3}$$

where α_s are coupling constants of scaling dimension $[\text{mass}]^{-2s}$.

3.1 CDD factors

It is known that the perturbation by the irrelevant operators $\alpha_s[T\bar{T}]_s$ simply modifies the original S-matrix by a CDD factor [12],

$$S^{(s)}_{\text{CDD}}(\theta) = e^{ig_s \sinh s\theta}, \tag{3.4}$$

where a dimensionless coefficient g_s is given by

$$g_s = -\alpha_s M^{2s}. \tag{3.5}$$

Being CDD, this additional S-matrix factor acts as a scalar factor which does not change the matrix structure. If the particles become massless, this relation changes by the massless

JHEP11(2024)078

scaling limit $\theta \to \hat{\theta} \pm \Lambda, \Lambda \to \infty, M \to 0$ with $Me^{\Lambda} = \widehat{M}$ finite as explained in (2.13). Then, the CDD S-matrices become

$$S_{\rm CDD}^{(s)RR} = S_{\rm CDD}^{(s)LL} = 1, \qquad S_{\rm CDD}^{(s)RL}(\theta) = \exp[i\hat{g}_s e^{s\theta}], \qquad S_{\rm CDD}^{(s)LR}(\theta) = \exp[i\hat{g}_s e^{-s\theta}]. \tag{3.6}$$

Here we replaced $\hat{\theta}$ with θ and defined

$$\hat{g}_s = -\alpha_s \widehat{M}^{2s}. \tag{3.7}$$

If we add these irrelevant operators to the deformed minimal model with $\Phi_{\rm pert}$ as in (3.3), the diagonal CDD factor S-matrix becomes

$$S_{\rm CDD}^{(\alpha)RL}(\theta) = \prod_{s=1}^{\infty} \exp[i\hat{g}_s e^{s\theta}], \tag{3.8}$$

which will modify only the RL and LR scattering processes. We use a super-index (α) to denote the set of coefficients α_s in (3.3). The resulting S-matrices that replace those in (2.14) and (2.16) are

$$S_p^{(\alpha)RR}(\theta) = S_p^{(\alpha)LL}(\theta) = S_p(\theta), \tag{3.9}$$

$$S_p^{(\alpha)RL}(\theta) = S_p^{(\alpha)LR}(-\theta) = S_{\rm CDD}^{(\alpha)RL}(\theta) \cdot S_p(\theta + \frac{ip\pi}{2}). \tag{3.10}$$

The theory (3.3) is described by these new RSOS massless S-matrices and a corresponding TBA equation. Since the CDD factors are scalar functions, the magnonic structure is the same as the TBA in (2.18) with an additional link between the two colored nodes in figure 3 by a kernel given by

$$\varphi_{RL}(\theta) = \varphi_{LR}(-\theta) = \frac{1}{i}\frac{\partial}{\partial\theta} \ln S_{\rm CDD}^{(\alpha)RL}(\theta). \tag{3.11}$$

These kernels depend on all possible sets of the parameters α_s. See appendix A for the derivation of these statements. We will choose such sets which will generate RG flows into some well-defined UV CFTs. For this, we can consider a much simplified version of the TBA, namely, a plateaux equation as used in [11].

3.2 TBA and UV complete theories

If the theory is UV complete, the TBA should have well-defined solutions in the $r \equiv \widehat{M}R \to 0$ limit where the pseudo-energies have constant values in a wide region centered at $\theta = 0$. Then, the TBA equations are reduced to much simpler algebraic equations between these plateaux values.[3]

These equations are given by

$$x_n = (1 + x_{n-1})^{1/2}(1 + x_{n+1})^{1/2}, \qquad n = 1, \cdots, p-3, \tag{3.12}$$

$$x_0 = (1 + x_1)^{1/2}(1 + x_{p-2})^{\mathsf{a}}, \qquad x_{p-2} = (1 + x_{p-3})^{1/2}(1 + x_0)^{\mathsf{a}}, \tag{3.13}$$

[3] If the UV theory is an irrational CFT, these plateaux may not appear. Even so, it turns out that these equations still give correct UV central charges.

JHEP11(2024)078

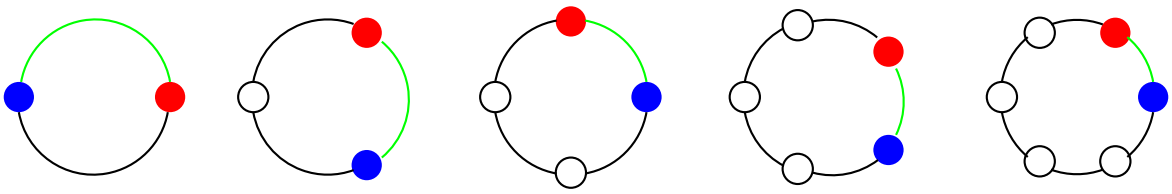


Figure 6. $\widehat{A}_{p-1}$ $(p = 3, 4, 5, 6, 7)$ affine Dynkin diagrams for new scattering theories with blue (R), red (L), and empty (magnons) nodes. The green links denote shifted universal kernels by α.

where we have defined

$$x_n \equiv e^{-\epsilon_n(0)}, \quad \mathsf{a} = \int_{-\infty}^{\infty} \varphi_{RL}(\theta)\, \frac{d\theta}{2\pi}. \tag{3.14}$$

This set of algebraic equations can be easily solved either numerically or even analytically depending on the exponent a. We need to find such a which gives real solutions since the pseudo energies should be real. It can be easily found that only $\mathsf{a} = 0, 1/2$ satisfy this condition. The $\mathsf{a} = 0$ case corresponds to the TBA (2.18) because no CDD factors are added. The S-matrices between L- and R-particles are given by (2.16).

If $\mathsf{a} = 1/2$, the TBA is described by the affine Dynkin diagram $\widehat{A}_{p-1}$ in figure 6. The CDD factor which satisfies the crossing-unitarity relation is given by

$$S^{RL}_{\rm CDD}(\theta) = S^{LR}_{\rm CDD}(-\theta) = -\tanh\left(\frac{\theta-\alpha}{2} - \frac{i\pi}{4}\right). \tag{3.15}$$

where α is a constant to be fixed later. The kernel associated with this is

$$\varphi_{RL}(\theta) = \varphi_{LR}(-\theta) = \frac{1}{\cosh(\theta-\alpha)}. \tag{3.16}$$

From eq. (3.14), the integration of this kernel gives $1/2$. Hence, we can have just one such CDD factor to get the real solution. Comparing with (3.8), we can find that the coefficients of the $[T\bar{T}]_s$ should be

$$\hat{g}_s = -2\, i^s\, e^{-s\alpha}, \quad \text{with} \quad s = \text{odd}. \tag{3.17}$$

While α is still an arbitrary parameter, it should be real to have real solutions for the pseudo-energies in the TBA. We present the $\alpha = 0$ case in this section and discuss the $\alpha \neq 0$ case in section 6 as they behave very differently. In the $\alpha = 0$ case the UV limit corresponds to a non-rational CFT, while for large α it exhibits roaming behaviours. This is similar to the relation between the sinh-Gordon and the staircase models in [18, 19], which formally corresponds to the $p = 3$ case here.

When $\alpha = 0$, φ_{RL} becomes the universal kernel and the TBA is the same as (2.18) with an additional link connecting the nodes 0 and $p-2$. A few cases of Dynkin diagrams are given in figure 6. These can be explicitly written as

$$\begin{aligned} \epsilon_a(\theta) &= \delta_{a0}\frac{r}{2}e^{\theta} + \delta_{a,p-2}\frac{r}{2}e^{-\theta} - \varphi \star \left[\ln\left(1+e^{-\epsilon_{a-1}}\right) + \ln\left(1+e^{-\epsilon_{a+1}}\right)\right](\theta), \\ \text{with} \quad \epsilon_a &\equiv \epsilon_{a+p-1}, \quad \text{for} \quad a = 0, \cdots, p-2. \end{aligned} \tag{3.18}$$

JHEP11(2024)078

Thanks to this additional link, the UV limit $r \to 0$ will be very different from (2.18). We will show in the next section that the UV CFT is the parafermionic Liouville field theory (PLFT) and the S-matrices (3.9), (3.10), and (3.15) are those of the parafermionic sinh-Gordon (PShG) model.

4 Parafermionic sinh-Gordon model

Parafermions (PFs) [20] appear in various two-dimensional QFTs. As fermions can generate supersymmetry, PFs can generate fractional supersymmetry [21]. In this section, we will focus on the PShG model which generalizes the ordinary sinh-Gordon and the supersymmetric (fermionic) sinh-Gordon (SShG) models.

4.1 The sinh-Gordon model

This simple integrable QFT has several interesting properties which are shared by both the SShG and PShG models. The sinh-Gordon model is an integrable QFT with a Lagrangian

$$\mathcal{L}_{\text{ShG}}(\Phi) = \frac{1}{4\pi}(\partial_a \phi)^2 + 2\mu \cosh 2b\phi. \tag{4.1}$$

This model can be viewed as a perturbed Liouville field theory (LFT)

$$\mathcal{L}_L(\Phi) = \frac{1}{4\pi}(\partial_a \phi)^2 + \mu\, e^{2b\phi}, \tag{4.2}$$

by a relevant operator $e^{-2b\phi}$ where b is the coupling constant and μ is a dimensionful parameter known as the cosmological constant. The LFT is a CFT with a central charge

$$c_L = 1 + 6Q^2, \qquad Q = b + \frac{1}{b}, \tag{4.3}$$

where Q is a background charge. The vertex operators

$$V_\alpha(x) = e^{2\alpha\phi(x)} \tag{4.4}$$

have conformal dimensions

$$\Delta_\alpha = \alpha(Q - \alpha). \tag{4.5}$$

If $\alpha = b$, the vertex operator $e^{2b\phi}$ has the holomorphic dimension 1 and becomes a screening operator.

Primary fields are given by (4.4) with $\alpha = \frac{Q}{2} + iP$ with arbitrary real P. Since the dimension becomes $Q^2/4 + P^2$, the two operators with $\alpha = \frac{Q}{2} \pm iP$ have the same dimension and can be identified up to a proportional constant, namely,

$$V_{Q/2-iP} = R_L(P) V_{Q/2+iP} \tag{4.6}$$

where $R_L(P)$ is known as the reflection amplitude which can be calculated from the two-point function

$$R_L(P) = (\pi\mu\gamma(b^2))^{-2iP/b} \frac{\Gamma(1 + 2iPb)\Gamma(1 + 2iP/b)}{\Gamma(1 - 2iPb)\Gamma(1 - 2iP/b)}, \tag{4.7}$$

with $\gamma(x) \equiv \Gamma(x)/\Gamma(1-x)$.

JHEP11(2024)078

The sinh-Gordon model can be described by an exact S-matrix between two scalar particles created by the field $\phi(x)$

$$S_{\rm ShG}(\theta) = \frac{\sinh\theta - i\sin\pi p}{\sinh\theta + i\sin\pi p}, \qquad p = \frac{b}{Q} = \frac{b^2}{1+b^2}. \tag{4.8}$$

The TBA of the sinh-Gordon model can be derived simply from this S-matrix

$$\epsilon(\theta) = mR\cosh\theta - \varphi_{\rm ShG} \star \ln\left(1+e^{-\epsilon}\right)(\theta) \tag{4.9}$$

where the kernel is a logarithmic derivative of $S_{\rm ShG}$

$$\varphi_{\rm shG}(\theta) = \frac{1}{\cosh\left(\theta - i\pi(p-\frac{1}{2})\right)} + \frac{1}{\cosh\left(\theta + i\pi(p-\frac{1}{2})\right)}. \tag{4.10}$$

As we will explain in the next section, both the reflection amplitudes and the TBA can be used to derive the scaling functions independently and can be shown to be identical. For this comparison, a relation between the mass m and the cosmological constant μ, known as the mass gap relation, is needed [17]

$$-\frac{\pi\mu}{\gamma(-b^2)} = \left[\frac{m}{4\sqrt{\pi}}\Gamma\left(\frac{1}{2(1+b^2)}\right)\Gamma\left(1+\frac{b^2}{2(1+b^2)}\right)\right]^{2+2b^2}. \tag{4.11}$$

Another relevant quantity is the bulk vacuum energy [22] given by

$$\mathcal{E} = \frac{m^2}{8\sinh\pi p}. \tag{4.12}$$

The reflection amplitude, the mass gap relation, and the vacuum energy can be used to compute the ground-state energy $E_0(R)$ independently from the TBA. This computation will provide cross-checks as we will explain later.

4.2 The SShG model

The $N=1$ supersymmetry maintains the integrability structure of the sinh-Gordon model. The supersymmetric Liouville field theory (SLFT) is given by

$$\mathcal{L}_{SL}(\Phi) = \frac{1}{4\pi}(\partial_\mu\phi)^2 - \frac{1}{\pi}(\psi\bar\partial\psi + \bar\psi\partial\bar\psi) + 4i\mu b^2\,\psi\bar\psi\, e^{2b\phi} + \pi\mu^2 b^2\, e^{4b\phi}. \tag{4.13}$$

The SLFT is a CFT with a central charge

$$c_{SL} = \frac{3}{2} + 6Q^2, \qquad Q = b + \frac{1}{2b}, \tag{4.14}$$

and the primary fields and their dimensions in the NS sector are given by

$$V_P^{\rm NS}(x) = e^{2\alpha\phi(x)}, \quad V_P^{\rm R}(x) = \sigma\, e^{2\alpha\phi(x)}, \qquad \alpha = \frac{Q}{2} + iP \tag{4.15}$$

which have conformal dimensions

$$\Delta_\alpha^{\rm NS} = \alpha(Q-\alpha) = \frac{Q^2}{4} + P^2, \tag{4.16}$$

JHEP11(2024)078

and an additional 1/16 for the R sector due to the twist field σ. The two operators $V_{\pm P}$ in both sectors are related by the reflection amplitudes [23, 24]

$$R_{SL}^{\rm NS}(P) = \left(\frac{\pi\mu}{2}\gamma\left(Qb\right)\right)^{-2iP/b} \frac{\Gamma(1+2iPb)\Gamma(1+iP/b)}{\Gamma(1-2iPb)\Gamma(1-iP/b)}, \tag{4.17}$$

$$R_{SL}^{\rm R}(P) = \left(\frac{\pi\mu}{2}\gamma\left(Qb\right)\right)^{-2iP/b} \frac{\Gamma\left(\frac{1}{2}+2iPb\right)\Gamma\left(\frac{1}{2}+iP/b\right)}{\Gamma\left(\frac{1}{2}-2iPb\right)\Gamma\left(\frac{1}{2}-iP/b\right)}. \tag{4.18}$$

The SShG model can be constructed in terms of the $N=1$ super-field $\Phi = \phi + \theta\psi + \bar{\theta}\bar{\psi} + \theta\bar{\theta}F$ with a super-potential $W(\Phi)$ which yields the Lagrangian

$$\mathcal{L}(\Phi) = \frac{1}{4\pi}(\partial_\mu\phi)^2 - \frac{1}{\pi}(\psi\bar{\partial}\psi + \bar{\psi}\partial\bar{\psi}) - \frac{i}{2\pi}\psi\bar{\psi}W''(\phi) + \frac{1}{4\pi}\left[W'(\phi)\right]^2. \tag{4.19}$$

If the superpotential is given by

$$W(\phi) = -4\pi\mu\cosh(2b\phi), \tag{4.20}$$

the potential energy is $(W')^2 \propto \sinh^2(2b\phi)$ which vanishes at $\phi = 0$. Therefore, the supersymmetry is exact and the on-shell massive particles respect the on-shell supersymmetry, which can be used to find the exact S-matrix of the model [25, 26].

However, another SShG model can be defined by a slightly different super-potential [10]

$$W(\phi) = -4\pi\mu\sinh(2b\phi). \tag{4.21}$$

This model shows dramatically different behaviour. Since $(W')^2 \propto \cosh^2(2b\phi) > 0$, the supersymmetry is spontaneously broken. The Goldstino, a massless fermion, survives stably in all scale while the bosonic particle created by ϕ becomes unstable and decays into the chiral (R- and L-moving) fermions as one can see from the $\psi\bar{\psi}\sinh(2b\phi)$ term in (2.13). We will focus on this massless SShG model.

Since there is no interactions between R-fermions (and L's), the S-matrix between LL or RR fermions are trivially

$$S_{\rm SShG}^{LL}(\theta) = S_{\rm SShG}^{RR}(\theta) = -1. \tag{4.22}$$

However, the S^{LR}-matrix between the L- and R-fermions is non-trivial. This can be determined by the crossing-unitarity relation

$$S_{\rm SShG}^{LR}(\theta)S_{\rm SShG}^{LR}(\theta+i\pi) = 1, \tag{4.23}$$

from which it is derived as

$$S_{\rm SShG}^{LR}(\theta) = \frac{\sinh\theta - i\sin\pi p}{\sinh\theta + i\sin\pi p}. \tag{4.24}$$

The constant p is related to the coupling constant b by

$$p = \frac{b}{Q} = \frac{2b^2}{1+2b^2}, \tag{4.25}$$

JHEP11(2024)078

with which the mass gap relation is expressed as

$$\pi\mu b^2\gamma(bQ) = \left(\frac{m}{8}\frac{\pi p}{\sin\pi p}\right)^{1+2b^2}. \tag{4.26}$$

The vacuum energy is given by the same result as (4.12).

This massless scattering theory describes the $p = 3$ (the Ising model) case of the RSOS models, where $S_{p=3} = -1$ being the scattering between non-interacting fermions and the S^{LR} is nothing but the CDD factor from the $[T\bar{T}]$ deformation in (3.15). The kernel connecting the R and L nodes in the TBA is again given by (4.10) where p is given by (4.25). Since it is shifted by imaginary constants, it is not compatible with the real shift α in (3.16) in general. Only exception arises when both shifts vanish at self-dual point. This corresponds to $\alpha = 0$ where the kernels connecting the two nodes of $\widehat{A}_2$ are identical in figure 6.

4.3 Parafermionic Sinh-Gordon models

Our main claim of this paper is that the S-matrices (3.9), (3.10), and (3.15) describe the parafermionic sinh-Gordon model for a generic integer k. So we will define the theory in details. The Lagrangian of the PLFT can be written as [27]

$$\mathcal{L}_{PL} = \mathcal{L}_{PF} + \frac{1}{4\pi}(\partial_\mu\phi)^2 - \mu\psi_1\overline{\psi}_1 e^{2b\phi} + \cdots, \tag{4.27}$$

where ψ_1 and $\overline{\psi}_1$ are $\mathbb{Z}_k$ parafermions with (anti-)holomorphic dimension $1 - 1/k$ and $\mathcal{L}_{PF}$ denotes the (formal) Lagrangian of the parafermionic CFT. The ellipsis includes counter terms whose exact expressions are not important in our study. This PLFT is also a CFT with a central charge

$$c_{PL} = \frac{3k}{k+2} + 6Q^2, \qquad Q = b + \frac{1}{kb}. \tag{4.28}$$

The primary fields are given by

$$V_P^{(n)}(x) = \sigma_n\, e^{2\alpha\phi}, \qquad \alpha = \frac{Q}{2} + iP, \quad n = 0, \cdots, k-1 \tag{4.29}$$

with the "spin field" σ_n. The dimension of this is given by

$$\Delta_n = \frac{Q^2}{4} + P^2 + \frac{n(k-n)}{2k(k+2)} \tag{4.30}$$

where the last term comes from the spin field. For the case of the SLFT ($k = 2$), two cases of $n = 0, 1$ correspond to the NS and R sectors, respectively.

The effective central charge is defined by $c_{\text{eff}} = c - 24\Delta_0$ with Δ_0 as a smallest dimension of the theory. For the PLFT, this is obtained by $n = 0$ and $P = 0$,

$$c_{\text{eff}} = \frac{3k}{k+2}. \tag{4.31}$$

For a generic integer k, we will focus on the $n = 0$ sector which is a generalization of the NS sector for the fractional supersymmetry where the dimension is still the same as (4.16).

JHEP11(2024)078

Two operators $V^{(0)}_{\pm P}$ are related by the reflection amplitude given by [27]

$$R^{(k)}_b(P) = e^{i\delta^{(k)}(P)} = \left(\frac{\pi\mu\gamma\left(b^2+\frac{1}{k}\right)}{k(k^2b^4)^{1/k}}\right)^{-\frac{2iP}{b}} \frac{\Gamma(1+2iPb)\Gamma\left(1+\frac{2iP}{kb}\right)}{\Gamma(1-2iPb)\Gamma\left(1-\frac{2iP}{kb}\right)}. \tag{4.32}$$

One can check that this reproduces (4.7) and (4.18) for $k = 1, 2$.

Now we can define the PShG models by adding integrable deformations to the PLFT

$$\mathcal{L}_{PL} = \mathcal{L}_{PF} + \frac{1}{4\pi}(\partial_\mu\phi)^2 - \mu\left(\psi_1\overline{\psi}_1 e^{2b\phi} + \eta\,\psi_1^\dagger\overline{\psi}_1^\dagger e^{-2b\phi}\right) + \cdots, \tag{4.33}$$

with the ellipsis including the counter terms. These models also have both massive and massless phases in the same way as the SShG model. The PShG model can be considered as the fractional sine-Gordon model, analysed in [21], with an imaginary coupling constant. Therefore, it has a fractional supersymmetry, which is a generalization of the supersymmetry. For the massive phase with $\eta = +$, the fractional supersymmetry is maintained, and the S-matrix describes scatterings among massive multiplets. On the other hand, if it is massless with $\eta = -$, the fractional supersymmetry is broken spontaneously and only massless PFs will be left to describe the theory.

The mass gap relation has been also computed in [27]:

$$\frac{\pi\kappa}{k}\gamma(bQ) = \left[\frac{m}{8\Gamma\left(\frac{k+2}{2}\right)}\Gamma\left(1+\frac{k^2b^2}{2(1+kb^2)}\right)\Gamma\left(\frac{k}{2(1+kb^2)}\right)\right]^{2bQ}, \tag{4.34}$$

and the vacuum energy is the same as (4.12) with $p = b/Q$.

We claim that the S-matrices between these massless particles are given by the RSOS S-matrices (2.14) and (3.15) with the self-dual coupling constant $b = 1/\sqrt{k}$. This will be justified by comparing scaling functions from the TBA with those obtained by the reflection amplitudes.

5 Comparing the TBA to the reflection amplitudes

In this section we compare the finite size ground-state energy coming from the reflection amplitudes to the same quantity coming from the TBA.

5.1 Effective central charge from the reflection amplitudes

In the parefermionic sinh-Gordon model the effective central charge is governed by the primary field with $n = 0$ and with the minimum value of the momentum P

$$c_{\text{eff}}(R) = \frac{3k}{k+2} - 24P^2 + \mathcal{O}(R). \tag{5.1}$$

Since the primary field is confined in Liouville potentials on both sides, the momentum is quantized by the condition

$$\delta^{(k)}(P) = \delta_1 P + \delta_3 P^3 + \cdots = \pi + 4QP\ln x, \qquad x = \frac{R}{2\pi}, \tag{5.2}$$

JHEP11(2024)078

where the reflection phase $\delta^{(k)}$ is defined in (4.32). At small volume the momentum can be expanded as

$$P = -\frac{\pi}{4Q\ln x} - \frac{\pi\delta_1}{16Q^2\ln^2 x} - \frac{\pi\delta_1^2}{64Q^3\ln^3 x} - \frac{\pi\delta_1^3+\pi^3\delta_3}{256Q^4\ln^4 x} + \dots \tag{5.3}$$

The corresponding effective central charge has a logarithmic volume dependence

$$c_{\text{eff}} = \frac{3k}{k+2} - \frac{3\pi^2}{2Q^2\ln^2 x} - \frac{3\pi^2\delta_1}{4Q^3\ln^3 x} - \frac{9\pi^2\delta_1^2}{32Q^4\ln^4 x} - \frac{3(2\pi^2\delta_1^3+\pi^4\delta_3)}{64Q^5\ln^5 x} + \dots \tag{5.4}$$

Observe that the $(\ln x)^{-1}$ term is missing.

The small P expansion takes the form

$$\delta^{(k)}(P) = -\frac{2P}{b}\ln\frac{\pi\mu\gamma\left(b^2+\frac{1}{k}\right)}{k(k^2b^4)^{1/k}} - 4PQ\gamma_E + P^3\zeta(3)\frac{16}{3}\left(b^3+\frac{1}{b^3k^3}\right) + \dots \tag{5.5}$$

In order to get the final form we still need to use the massgap relation (4.34). Let us note that the mass appears only at the linear order as

$$\delta^{(k)}(P) = -4PQ\ln m + \dots \tag{5.6}$$

which nicely combines with R to the dimensionless volume $mR = r$.

In order to compare with the TBA analysis we specify the results for the self dual point, defined by

$$b^2 = \frac{1}{k}; \qquad Q = \frac{2}{\sqrt{k}}. \tag{5.7}$$

The mass gap relation simplifies considerably

$$\frac{\pi\mu}{k}\gamma(2/k) = \left[\frac{m\Gamma^2(\frac{k}{4})}{16\Gamma(\frac{k}{2})}\right]^{4/k} \tag{5.8}$$

and the reflection factor

$$e^{i\delta(P)} = \left(\frac{m\Gamma^2\left(\frac{k}{4}\right)}{16\Gamma\left(\frac{k}{2}\right)}\right)^{-\frac{8iP}{\sqrt{k}}} \frac{\Gamma\left(1+\frac{2iP}{\sqrt{k}}\right)^2}{\Gamma\left(1-\frac{2iP}{\sqrt{k}}\right)^2}. \tag{5.9}$$

The small P expansion of the phase at the self dual point is

$$\delta^{(k)}(P) = \delta_1 P + \delta_3 P^3 + \dots = -\frac{8}{\sqrt{k}}\ln\left(\frac{m\Gamma^2\left(\frac{k}{4}\right)}{16\Gamma\left(\frac{k}{2}\right)}\right)P - 8\frac{\gamma_E}{\sqrt{k}}P + \frac{32\zeta(3)}{3k^{\frac{3}{2}}}P^3 + \dots. \tag{5.10}$$

Plugging back these values into eq. (5.4) and taking into account that $x = R/2\pi$ leads to the coefficients in table 1. We compare these numbers with the same quantities obtained by numerically solving the TBA equations.

JHEP11(2024)078

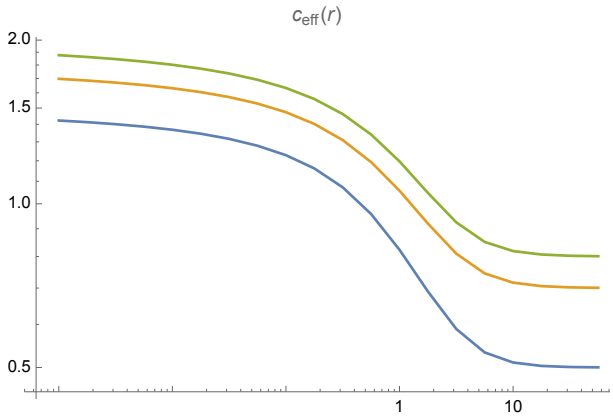


Figure 7. Logarithmic plot of the effective central charge as the function of the dimensionless volume $r = \widehat{M}R$ for $k = 2, 3, 4$ (blue,orange,green).

5.2 Numerical solution of the TBA

We solve the TBA equations (3.18), by discretizing the pseudo energies ϵ_a and performing the convolutions using discrete Fourier transforms. Iterating the equations until reaching the prescribed precision, (which we choose to be 10^{-16}), leads to the effective central charge $c_{\text{eff}}(r)$ as the function of the dimensionless volume $r = \widehat{M}R$, which serves as the RG parameter. We present the results for the $k = p - 1 = 2, 3, 4$ cases. The behaviour of the effective central charge is displayed on figure 7.

In the IR, i.e. for large volumes R, the left and right movers decouple and we get back the IR minimal model CFT with central charge $c_{\text{IR}} = 1 - \frac{6}{(k+1)(k+2)}$. By investigating the numerical solution one can observe that the non-trivial behaviour is concentrated on the small and large θ region. In each domain one of the colored nodes (with the driving term ϵ_0 or ϵ_{p-2}) becomes negligible. The TBA is then no longer the ring, rather the line, which describes the same left or right moving scattering theories (2.15).

In the UV, the effective central charge approaches its UV value $c_{\text{UV}} = \frac{3k}{k+2}$ very slowly. The reason is that in the central domain the functions $L_i(\theta) = \log(1 + e^{-\epsilon_i(\theta)})$ does not approach any plateaux value, see figure 8. Indeed in this limit the driving terms are negligible and the central behaviour is governed by the same function we would have in the sinh-Gordon theory at the self dual point, where it is well-known that the effective central charge approaches its UV value logarithmically. We have already obtained this logarithmic behaviour in our case, which we try to fit numerically now. We thus parametrize the small volume behaviour of the central charge as

$$c_{\text{eff}}(r) = \frac{3k}{k+2} + \sum_{n=2} \frac{c_n(k)}{(\log r)^n} + O(r) \tag{5.11}$$

by focusing on the logarithmic corrections and neglecting any higher order polynomials in r. We extract the coefficients $c_n(k)$ numerically, by fitting $c_{\text{eff}}(r)$ in the range $10^{-10} - 10^{-6}$. The results are displayed in the table 1 and shows a convincing agreement with the analytically obtained expressions from the reflection factors.

JHEP11(2024)078

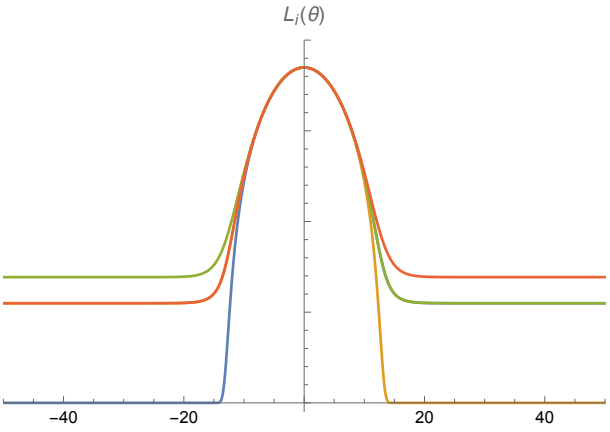


Figure 8. Plot of the $L_i = \log(1 + e^{-\epsilon_i})$ functions for $k = 4$ and dimensionless volume $r = 10^{-5}$ as the function of θ. The functions $\{L_0, L_1, L_2, L_3\}$ correspond to {blue,orange,green,red). Clearly $L_i(\theta) = L_{3-i}(-\theta)$.

	c_2	c_3	c_4	c_5
$k = 2$	7.402199	42.7620	185.218	714.563
	7.402203	42.7628	185.282	717.247
$k = 3$	11.10332	77.8573	409.598	1924.84
	11.10330	77.8543	409.425	1919.36
$k = 4$	14.8045	119.428	722.797	3898.75
	14.8044	119.4197	722.475	3892.55

Table 1. Numerically fitted coefficients in the various cases above and their analytical expressions from the reflection amplitudes, below.

The agreement we found tests not only the approach based on the reflections factors of the PShG model, but specifically its mass gap relation and the first two coefficients δ_1, δ_3.

6 Roaming TBA

So far we have considered the S^{RL} and S^{LR} matrices given by (3.15) with $\alpha = 0$. For the case of $\alpha \neq 0$, the S^{RL} and S^{LR} are changed by a shift α in the arguments. The TBA can be derived from the same set of massless S-matrices as

$$\epsilon_a(\theta) = -\varphi \star \left[\ln\left(1 + e^{-\epsilon_{a-1}}\right) + \ln\left(1 + e^{-\epsilon_{a+1}}\right)\right](\theta), \quad a = 1, \cdots, p-3, \tag{6.1}$$

$$\epsilon_0(\theta) = \frac{r}{2}e^{\theta} - \varphi \star \ln\left(1 + e^{-\epsilon_1}\right) + \varphi^{(+)} \star \ln\left(1 + e^{-\epsilon_{p-2}}\right)(\theta), \tag{6.2}$$

$$\epsilon_{p-2}(\theta) = \frac{r}{2}e^{-\theta} - \varphi \star \ln\left(1 + e^{-\epsilon_{p-3}}\right) + \varphi^{(-)} \star \ln\left(1 + e^{-\epsilon_1}\right)(\theta), \tag{6.3}$$

with kernels $\varphi^{(\pm)}$ defined by

$$\varphi^{(\pm)}(\theta) = \varphi(\theta \pm \alpha) \tag{6.4}$$

and with the same graph in figure 6.

JHEP11(2024)078

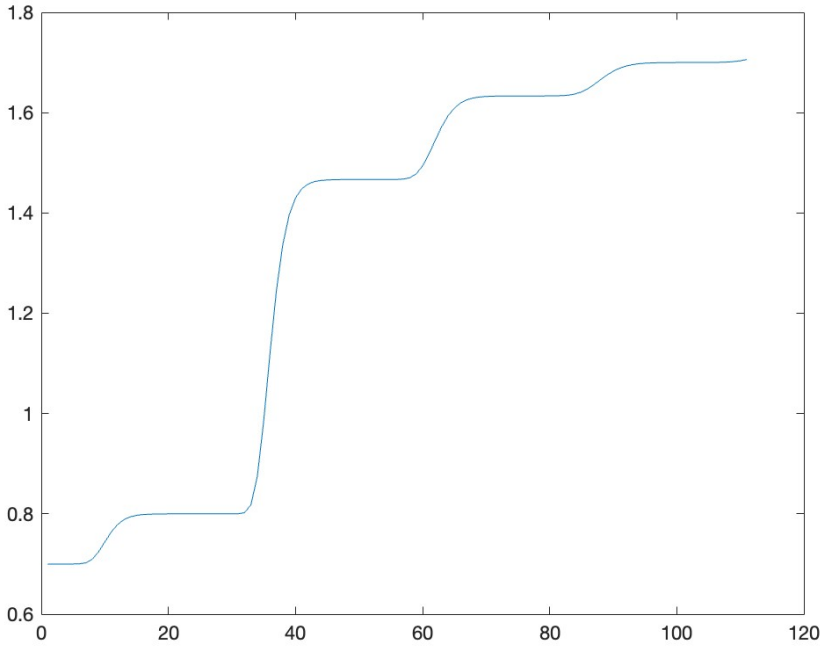


Figure 9. $c_{\text{eff}}(r)$ vs $-\log r$ for $p = 4$ with $\alpha = 10\pi$.

This TBA with real α can be mapped to the some of the TBA systems conjectured in [28, 29] to describe roaming trajectories between coset minimal models. Although the kernels in [28, 29] are apparently different, they can be transformed to those in (6.3) by shifting the rapidities in the definition of the pseudo energies and by redefining the scale r appropriately. This result implies that the massless S-matrices in (3.9), (3.10), and (3.15) are the exact S-matrices behind the conjectured roaming TBA of the $\mathbb{Z}_k$ PF minimal series.

Although the roaming behaviour was analyzed thoroughly in the more general cases in [28, 29], we just present here our findings, which also confirm their results. For sufficiently large $\alpha \gg 1$, this TBA is showing interesting roaming trajectories ($p = k + 1$):

$$\mathcal{M}_{k+1} \to \mathbb{Z}_k\mathcal{M}_1 \to \mathbb{Z}_k\mathcal{M}_{k+1} \to \mathbb{Z}_k\mathcal{M}_{2k+1} \to \cdots, \tag{6.5}$$

where we denote the $\mathbb{Z}_k$ PF minimal series by $\mathbb{Z}_k\mathcal{M}_\ell$ ($\ell = 1, 2, \cdots$) which can be written as coset CFTs as follows:

$$\mathbb{Z}_k\mathcal{M}_\ell = \frac{su(2)_k \otimes su(2)_\ell}{su(2)_{k+\ell}}, \qquad \text{with} \quad c = \frac{3k\ell(k+\ell+4)}{(k+2)(\ell+2)(k+\ell+2)}. \tag{6.6}$$

For example, as shown in figure 9 for the $p = 4$ case, the starting IR CFT has $c_{IR} = 0.7$ of the $\mathcal{M}_4$ CFT. The next central charge jumps to $c = \frac{4}{5}$ which is the first CFT in $\mathbb{Z}_3$ PF minimal series and succeeded by $c = \frac{22}{15}, \frac{49}{30}, \cdots$.

Among many interesting TBA systems proposed in [28, 29], only a subset has been reproduced from our S-matrix approach. It would be interesting to extend this approach to the general cases, not only in the roaming limit but also for other values of the parameters which may appear in the RL scatterings.

JHEP11(2024)078

7 Conclusion

QFTs that interpolate between two CFTs in their UR and IR limits are valuable but rare examples from which we can understand quantitatively how fundamental degrees of freedom such as operators and on-shell particles are connected. In this paper, we have approached to find new QFTs from the IR point of view based on the exact massless S-matrices which are deformed by $[T\bar{T}]$. These special irrelevant fields preserve integrability and modify the S-matrices between R- and L-particles in a systematic way. Generalizing [11], we have applied $[T\bar{T}]$ deformations on non-diagonal kink scattering theories of the perturbed minimal CFTs $\mathcal{M}_p$. We have found fine-tuned $[T\bar{T}]$ deformations that can be UV complete. Our main finding is the $\mathbb{Z}_{p-1}$ PShG model with the self-dual coupling constant which leads to the $\mathbb{Z}_{p-1}$ PF LFTs in the UV limit. This extends the previous result, which connects the super Liouville theory to the critical Ising model [10] and contains it as its simplest example. We have tested this conjecture thoroughly by comparing the UV limit of the TBA equations with the reflection factors of the UV conformal field theory. It is remarkable to see how a fractional supersymmetry associated with the $\mathbb{Z}_{p-1}$ PF emerges from the simple minimal CFT $\mathcal{M}_p$ by the fined tuned irrelevant $[T\bar{T}]$ deformations. This emergent symmetry generalizes the phenomena observed in the Ising model ($p = 3$) [10].

By choosing the real parameter in the CDD factor very large, we obtained the $\mathbb{Z}_{p-1}$ parafermionic minimal CFT series with roaming trajectories and recovered a conjectured flow of [28, 29]. It is important to emphasize that the UV behaviour depends quantitatively on the parameter α. In particular, it would be very interesting to investigate the UV limit for purely imaginary α. We think that it should correspond to the $\mathbb{Z}_{p-1}$ PShG models away from the self-dual couplings, but further research is needed to decide about this question.

We want to emphasize once more that our TBAs have been derived from exact massless S-matrices rather than many educated guesses on TBAs and non-linear integral equations in the literature. (See [9, 31] and references therein.) In addition, we have also derived two of previously conjectured TBAs, one in figure 5 and the PF roaming TBA, from the exact S-matrices. It would be nice if we can prove other conjectured TBAs in this way.

In this work, we have considered the $\mathcal{M}_p$ CFT as a scattering theory of RSOS kinks based on the $\Phi_{1,3}$ deformation and mapped the space of all integrable irrelevant perturbations with a UV limit. In fact, there are other integrable descriptions of the same minimal CFTs related to different integrable deformations. It would be interesting to find new UV CFTs based on these different S-matrices associated with the same IR minimal CFTs. In this way, we may lead to a complete classification of UV complete theories for a given IR CFT.

Massless scattering theories gain attentions recently related to the world-sheet S-matrices of AdS3/CFT2 duality [30]. Being CFTs, these S-matrices are between RR and LL particles while RL scatterings are trivial. It will be interesting to consider non-trivial RL scatterings, possibly related to the $[T\bar{T}]$ deformations and their RG flows in the context of AdS/CFT duality. Another interesting direction is to understand relations between these new RG flows and non-invertible symmetries associated with some topological defect lines [32].

JHEP11(2024)078

Acknowledgments

We want to thank J. Balog, P. Dorey, M. Lencses, F. Ravanini for valuable discussions and comments. CA thanks the mathematical physics group of Matthias Staudacher at Humboldt University in Berlin and Wigner Institute in Budapest and ZB thanks Ewha University for hospitality where parts of this work have been performed. In particular, CA acknowledges partial support of his stay by the *Kolleg Mathematik Physik Berlin* (KMPB). This work was supported in part by the government of the Republic of Korea (MSIT) and the National Research Foundation of Korea (NRF-2023K2A9A1A01098567) for the Mobility program between Korea and Hungary, by (NRF-2016R1D1A1B02007258) (CA), and by the K134946 NKFIH Grant.

JHEP11(2024)078

A Magnonic scatterings with a CDD factor

In this appendix we investigate how a CDD factor modifies the TBA equations with magnons. We do the calculations for theories with one or two distinguished (massive) nodes and M magnons.

A.1 Massive scattering

Let us start with just one single type of massive particles which scatters on itself with a non-diagonal scattering matrix $S(\theta) = S_0(\theta)R(\theta)$, where $R(\theta)$ solves the Yang-Baxter equation, typically a Boltzman weight in an integrable lattice model and $S_0(\theta)$ is a scalar factor, which ensures unitarity and crossing symmetry. In determining the finite volume spectrum the Bethe Yang equations have to be solved

$$e^{ip(\theta_j)L}\prod_{k\neq j} S(\theta_j-\theta_k)\Psi(\theta_1,\dots,\theta_n) = e^{ip(\theta_j)L}\prod_{k\neq j} S_0(\theta_j-\theta_k)\Lambda_\Psi\Psi(\theta_1,\dots,\theta_n). \tag{A.1}$$

It involves the diagonalization of the lattice transfer matrix and with its eigenvalue, Λ_Ψ, the momentum quantization can be formulated as

$$e^{ip(\theta_j)L}\prod_{k\neq j} S_0(\theta_j-\theta_k)\Lambda_\Psi = 1. \tag{A.2}$$

In diagonalizing the lattice transfer matrix

$$\mathbb{T}(\theta|\theta_1,\dots,\theta_n) = \mathrm{tr}_0(\prod R(\theta-\theta_j)) \tag{A.3}$$

one typically uses the method of (nested) Bethe ansatz. In the rank one case it involves just a single type of magnonic particles, while for higher rank theories more magnons are needed. In order to describe all states one also has to investigate the magnon-magnon scatterings, classify their bounds-states and calculate their scattering matrices, i.e. the magnonic bootstrap has to be closed. In the following we assume that there are M magnons and that they scatter on each other by the $S_{nm}(\theta)$ scattering factor, $n, m = 1, \dots, M$.

The finite volume spectrum can be calculated as if it were a diagonally scattering theory. We place both physical and magnonic particles and demand the periodicity of their wave function. Let us denote the massive particle with the label 0 and the massive-massive

scattering by $S_{00}(\theta) = S_0(\theta)$, where we assumed a specific normalization for the lattice R matrix. The magnon scatters on the massive particle as $S_{n0}(\theta)$ while the massive particle on the magnon as $S_{0n}(\theta)$. These S-matrix elements are not independent. The $S_{00}(\theta)$ scattering is connected to the $S_{0n}(\theta)$ and $S_{n0}(\theta)$ scatterings by crossing symmetry [33], while $S_{nm}(\theta)$ are related to $S_{11}(\theta)$ by bootstrap or symmetry relations.

Let us place on the circle N particles of type $n_1, \dots, n_N$ and rapidities $\theta_{n_1}, \dots, \theta_{n_N}$. The Bethe Yang equation at the magnonic language reads as

$$e^{ip_{n_j}(\theta_j)L} e^{i\delta} \prod_{k \neq j} S_{n_j n_k}(\theta_{n_j} - \theta_{n_k}) = 1 \tag{A.4}$$

where $p_{n_j}(\theta)$ denotes the momentum of the particle of type n_j. For massive particles $p_0(\theta) = p(\theta) = m \sinh \theta$, while for magnons $p_n(\theta) = 0$. We also included a possible phase factor $e^{i\delta}$ which typically has no effect in the thermodynamic limit.

In the thermodynamic limit we can introduce the densities of the particles of type n as ρ_{n_j} and their hole densities as $\bar{\rho}_{n_j}$. The thermodynamic limit of the Bethe Yang equations reads as

$$\rho_{n_j} + \bar{\rho}_{n_j} = p'_{n_j} L + \sum_k \phi_{n_j n_k} \star \rho_{n_k} \tag{A.5}$$

where $p'_{n_j}(\theta) = \partial_\theta p_{n_j}(\theta)$, $\phi_{n_j n_k}(\theta) = -i\partial_\theta \log S_{n_j n_k}(\theta)$ and $\star$ denotes the convolution. Let us spell out the details by specifying n_j to 0 and $n = 1, \dots, M$:

$$\begin{aligned} \rho_0 + \bar{\rho}_0 &= p' L + \phi_{00} \star \rho_0 + \sum_{n=1}^{M} \phi_{0n} \star \rho_n \\ \rho_n + \bar{\rho}_n &= \phi_{n0} \star \rho_0 + \sum_{m=1}^{M} \phi_{nm} \star \rho_m . \end{aligned} \tag{A.6}$$

In many of the theories the bootstrap or symmetry relations between the various magnons and their boundstates imply that

$$(\delta_{nm} - \phi_{nm})^{-1} = \delta_{nm} - (\delta_{n+1m} + \delta_{n-1m}) s \tag{A.7}$$

for $M \geq n, m > 0$, where

$$s(\theta) = \frac{1}{\cosh(\theta)} \tag{A.8}$$

Using this relation the magnonic equations simplify to

$$\begin{aligned} \rho_n + \bar{\rho}_n &= s \star (\bar{\rho}_{n+1} + \bar{\rho}_{n-1}) + (\phi_{n0} - s \star (\phi_{n+10} + \phi_{n-10})) \star \rho_0 \\ &= s \star (\bar{\rho}_{n+1} + \bar{\rho}_{n-1}) + \delta_{n1} s \star \rho_0 . \end{aligned} \tag{A.9}$$

Here we also used that ϕ_{n0} satisfies the bootstrap or symmetry equation and $\phi_{10} - s \star \phi_{20} = s$. Finally we can write

$$\begin{aligned} \rho_0 + \bar{\rho}_0 &= p' L + \phi_{00} \star \rho_0 + \phi_{01} \star (s \star \rho_0) + \sum_n \phi_{0n} \star (-\bar{\rho}_n + s \star (\bar{\rho}_{n+1} + \bar{\rho}_{n-1})) \\ &= p' L + s \star \bar{\rho}_1 \end{aligned} \tag{A.10}$$

JHEP11(2024)078

where we used the equations related to the crossing symmetry [33] and the bootstrap or symmetry equations

$$\phi_{00} + \phi_{01} \star s = 0\,; \qquad -\phi_{01} + \phi_{02} \star s = s. \tag{A.11}$$

Here and from now on all sums go from 1 to M, i.e. $\sum_n \equiv \sum_{n=1}^{M}$. The diagram, which encodes the corresponding TBA system is in figure 2. This is a typical TBA system, which appears in many models. In particular, for the minimal model perturbed with $\Phi_{1,3}$ we have $M = p - 3$.

A.2 Massless scattering and its irrelevant perturbations

Let us now assume that we have two different distinguished nodes. We denote the new node by $\bar{0}$. This situation corresponds to a CFT when we have the right movers with $p_0 = me^{\theta}$ and the left movers with $p_{\bar{0}} = -me^{-\theta}$ and can be obtained as the zero mass limit of the previous scattering theory. In the CFT the left-left and the right-right scatterings are equivalent to the scatterings above, while the left-right scattering is the identity. This implies that we have separate magnons for left and right movers. We distinguish the magnons of the left movers by a bar, although their kernels are the same as the unbared onces, i.e. $\phi_{\bar{0}\bar{0}} = \phi_{00}, \phi_{\bar{0}\bar{n}} = \phi_{0n}$. We can repeat the calculations above resulting two decoupled systems, each looking the same as the massive one. The only difference is in the driving terms $p'_0 = me^{\theta}$ and $p'_{\bar{0}} = me^{-\theta}$. The corresponding diagram is in figure 3.

In the following we introduce irrelevant perturbations which drives the theory away from the IR fix point. We focus on integrable perturbations which can be described by coupling the left movers and the right movers by non-trivial scatterings, which satisfy the Yang-Baxter equation.

A.2.1 Identity type perturbation

Let us assume now that we couple the left and right movers with a CDD factor

$$S^{LR}(\theta) = S_{0\bar{0}}(\theta)\mathbb{I}. \tag{A.12}$$

This simple scattering do not effect the magnons merely couples the 0 and $\bar{0}$ indices as

$$\rho_0 + \bar{\rho}_0 = p'_0 L + \phi_{00} \star \rho_0 + \sum_n \phi_{0n} \star \rho_n + \phi_{0\bar{0}} \star \rho_{\bar{0}} \tag{A.13}$$

and an analogous equation for the $\bar{0}$ particle

$$\rho_{\bar{0}} + \bar{\rho}_{\bar{0}} = p'_{\bar{0}} L + \phi_{00} \star \rho_{\bar{0}} + \sum_n \phi_{0n} \star \rho_{\bar{n}} + \phi_{\bar{0}0} \star \rho_0. \tag{A.14}$$

Since the previous kernels do not change we can repeat our simplifying manipulations to bring the TBA in the form

$$\rho_0 + \bar{\rho}_0 = p'_0 L + s \star \bar{\rho}_1 + \phi_{0\bar{0}} \star \rho_{\bar{0}}\,; \qquad \rho_{\bar{0}} + \bar{\rho}_{\bar{0}} = p'_{\bar{0}} L + s \star \bar{\rho}_{\bar{1}} + \phi_{\bar{0}0} \star \rho_0. \tag{A.15}$$

Clearly the new coupling between the left and right distinguished nodes did not participate in the cancellations and survived the simplifying manipulations. The resulting TBA system can be encoded into the Dynkin diagram, in which the two colored nodes on figure 3 are coupled. Although the coupling between 0 and $\bar{0}$, namely $\phi_{0\bar{0}}$ can be different from s.

JHEP11(2024)078

A.2.2 Same S-matrix type perturbation

Let us assume now that we couple the left and right movers with the same scattering matrix as the left-left and right-right scatterings, see also eq. (2.20)

$$S^{LR}(\theta) = S(\theta). \tag{A.16}$$

In this case left and right movers share the same magnons, $\rho_n \equiv \rho_{\bar{n}}$ and the diagonalization of the transfer matrix leads to the following equations

$$\begin{aligned}
\rho_0 + \bar{\rho}_0 &= p_0' L + \phi_{00} \star (\rho_0 + \rho_{\bar{0}}) + \sum_n \phi_{0n} \star \rho_n \\
\rho_{\bar{0}} + \bar{\rho}_{\bar{0}} &= p_{\bar{0}}' L + \phi_{00} \star (\rho_0 + \rho_{\bar{0}}) + \sum_n \phi_{0n} \star \rho_n \\
\rho_n + \bar{\rho}_n &= \phi_{n0} \star (\rho_0 + \rho_{\bar{0}}) + \sum_m \phi_{nm} \star \rho_m .
\end{aligned} \tag{A.17}$$

Using similar manipulations as above we can arrive at the TBA equations encoded in the diagram on figure 5.

By introducing an extra CDD factor between the left and right scatterings

$$S^{LR}(\theta) = S_{0\bar{0}}(\theta) S(\theta) \tag{A.18}$$

we can repeat the previous calculation which introduces a new connection between the 0 and $\bar{0}$ nodes

$$\rho_0 + \bar{\rho}_0 = p_0' L + \phi_{00} \star (\rho_0 + \rho_{\bar{0}}) + \sum_n \phi_{0n} \star \rho_n + \phi_{0\bar{0}} \star \rho_{\bar{0}} \tag{A.19}$$

and similar equation for $\bar{0}$, without affecting the magnonic equations. After the previous simplification is applied, TBA is given by a diagram in which figure 5 has an extra link between the 0 and $\bar{0}$ nodes. This diagram does not correspond to a Dynkin diagram so we do not expect a sensible UV limit.

A.2.3 Shifted S-matrix type perturbation

Let us finally investigate the case when the left-right scattering is the appropriately shifted left-left scattering, see also eq. (2.16)

$$S^{LR}(\theta) = \bar{S}_0(\theta) S(\theta + i\alpha) = S_{0\bar{0}}(\theta) R(\theta + i\alpha) \tag{A.20}$$

In this case we have to diagonalize an appropriately shifted inhomogenous transfer matrix. Left and right movers share the same magnons, but they couple to them in a different way. Choosing the shift appropriately, can introduce the identifications in the magnons as $\rho_{\bar{n}} \equiv \rho_{M+1-n}$ and gives

$$\begin{aligned}
\rho_0 + \bar{\rho}_0 &= p_0' L + \phi_{00} \star \rho_0 + \phi_{0\bar{0}} \star \rho_{\bar{0}} + \sum_n \phi_{0n} \star \rho_n \\
\rho_{\bar{0}} + \bar{\rho}_{\bar{0}} &= p_{\bar{0}}' L + \phi_{00} \star \rho_{\bar{0}} + \phi_{\bar{0}0} \star \rho_0 + \sum_{\bar{n}} \phi_{0n} \star \rho_{\bar{n}} \\
\rho_n + \bar{\rho}_n &= \phi_{n0} \star \rho_0 + \phi_{n\bar{0}} \star \rho_{\bar{0}} + \sum_m \phi_{nm} \star \rho_m .
\end{aligned} \tag{A.21}$$

JHEP11(2024)078

Using the kernel identities, the TBA equations can be simplified, which leads to the TBA diagram on figure 4. Here it was assumed that $\bar{S}_0(\theta)$ was chosen such a way, that the direct coupling between the distinguished nodes 0 and $\bar{0}$ disappears. This can be done as it is shown in the explicit example below (A.44), requiring that

$$\phi_{0\bar{0}} + \phi_{0M} \star s = 0\,; \qquad \phi_{\bar{0}0} + \phi_{M0} \star s = 0. \tag{A.22}$$

Let us now introduce an extra CDD factor between the left-right scatterings

$$S^{LR}(\theta) = \bar{S}_{0\bar{0}}(\theta)\bar{S}_0(\theta)S(\theta + i\alpha). \tag{A.23}$$

This modifies the TBA equations as

$$\rho_0 + \bar{\rho}_0 = p_0' L + \phi_{00} \star \rho_0 + (\phi_{0\bar{0}} + \bar{\phi}_{0\bar{0}}) \star \rho_{\bar{0}} + \sum_n \phi_{0n} \star \rho_n \tag{A.24}$$

and similar equation for $\bar{0}$. Using again the kernel identities we can simplify the TBA equations. The effect of the CDD factor is to introduce an extra coupling between the nodes 0 and $\bar{0}$, which can be different than s. The effective diagram is the circle diagram shown on figure 6, where the green links indicate the kernel $\bar{\phi}_{0\bar{0}}$ of the CDD factor.

A.2.4 Comments

Let us summarize what we found. We investigated IR conformal field theories perturbed irrelevantly by coupling the left and right movers in an integrable way. We focused on the effect of introducing an extra CDD factor in the scatterings between left and right movers. We found that an extra coupling appears in the TBA description between the distinguished nodes, which is related to the logarithmic derivative of the CDD factor. Our derivation was very general and did not rely on the explicit form of the kernels. If a simplification appears in the original TBA describing the irrelevant perturbation, then the same simplification appears also with the CDD factor and the only effect is the extra coupling between the distinguished nodes. In the next subsection we provide explicit formulas, how it happens in the minimal models perturbed by $\Phi_{1,3}$.

A.3 Minimal models perturbed with $\Phi_{1,3}$

The previous considerations were quite general valid for any scattering theories with the same magnonic structure.

In applying it to the minimal models perturbed by $\Phi_{1,3}$ we have to recall the diagonalization of the RSOS transfer matrices, which was done in [34] for the homogenous case. It involves one single magnon and by extending it to the inhomogenous case we arrive at

$$\prod_{j=1}^{N} \frac{\sinh\mu(\alpha_k - \theta_j + \frac{i\pi}{2})}{\sinh\mu(\alpha_k - \theta_j - \frac{i\pi}{2})} = \omega^2(-1)^{N+1} \prod_{m=1}^{N/2} \frac{\sinh\mu(\alpha_k - \alpha_m + i\pi)}{\sinh\mu(\alpha_k - \alpha_m - i\pi)} \tag{A.25}$$

JHEP11(2024)078

where we rescaled the roots of the magnon rapidities α_k compared to [], $\mu = \frac{1}{p}$ and ω is a constant phase. The transfer matrix eigenvalue with these roots take the form

$$\Lambda(\theta|\theta_1,\dots,\theta_n,\alpha_1,\dots,\alpha_m) = \omega\prod_j \sinh\mu(\theta-\theta_j-i\pi)\prod_k \frac{\sinh\mu(\theta-\alpha_k+\frac{i\pi}{2})}{\sinh\mu(\theta-\alpha_k-\frac{i\pi}{2})} + \omega^{-1}\prod_j \sinh\mu(\theta-\theta_j)\prod_k \frac{\sinh\mu(\theta-\alpha_k-\frac{3i\pi}{2})}{\sinh\mu(\theta-\alpha_k-\frac{i\pi}{2})}. \tag{A.26}$$

From these Bethe ansatz equations we can extract the magnon-magnon scatterings

$$S_{11}(\alpha) = \frac{\sinh\mu(\alpha+i\pi)}{\sinh\mu(\alpha-i\pi)} \equiv [2] \tag{A.27}$$

where we have introduced the notation

$$[n] = \frac{\sinh\mu(\alpha+n\frac{i\pi}{2})}{\sinh\mu(\alpha-n\frac{i\pi}{2})}. \tag{A.28}$$

With this notation the magnon-massive scattering is simply $S_{10}(\alpha) = [-1]$. The magnon-magnon scattering is attractive, with a pole at $\alpha = i\pi$, implying that magnons can form boundstates. The simplest boundstate is a two string with $\alpha \pm i\frac{\pi}{2}$. The scattering of this two string labeled by 2 can be bootstrapped as

$$S_{12}(\alpha) = S_{11}\left(\alpha+\frac{i\pi}{2}\right)S_{11}\left(\alpha-\frac{i\pi}{2}\right) = [1][3]. \tag{A.29}$$

Similarly, the magnon scatters on the boundstate with $S_{20}(\alpha) = [-2]$. Following this procedure one arrives at an n-string $\left\{\alpha+\frac{i\pi(n-1)}{2}, \alpha+\frac{i\pi(n-3)}{2}, \dots, \alpha-\frac{i\pi(n-3)}{2}, \alpha-\frac{i\pi(n-1)}{2}\right\}$ with scatterings

$$S_{1n}(\alpha) = [n-1][n+1]\,; \qquad S_{n0}(\alpha) = [-n]. \tag{A.30}$$

Recalling that $\mu = 1/p$ and inspecting the scatterings one can see that the last string we can form is with $n = p-1$. Indeed its scatterings are

$$S_{1p-1}(\alpha) = -[p-2]\,; \qquad S_{p-10}(\alpha) = [1-p] = -\frac{\cosh\mu(\alpha+\frac{i\pi}{2})}{\cosh\mu(\alpha-\frac{i\pi}{2})}. \tag{A.31}$$

To complete the whole picture we should calculate the scattering of a general n-string on an m-string:

$$S_{nm}(\alpha) = [n-m][n-m+2]^2\dots[n+m-2]^2[n+m] \tag{A.32}$$

where we assumed that $n \geq m$.

Let us also point out that from the transfer matrix eigenvalue we can extract the massive-magnon scattering which turns out to be the inverse of the magnon-massive scattering

$$S_{0n} = [n] = S_{n0}^{-1} = [-n]^{-1}. \tag{A.33}$$

This is related to the fact that we have to choose between the BA for the magnons and its inverse such a way that the magnon densities will be positive in the thermodynamic limit.

JHEP11(2024)078

A.3.1 Kernels in the TBA

In calculating the groundstate energy we will need the logarithmic derivative of the kernels $\phi(\theta) = -i\partial_\theta \log S(\theta)$. Performing the calculations we found

$$\phi_{nm} = (n-m) + 2(n-m+2) + \cdots + 2(n+m-2) + (n+m)\,; \qquad \phi_{n0} = -(n) \tag{A.34}$$

where

$$(n) = i\mu \coth\mu\left(\alpha - \frac{in\pi}{2}\right) - i\mu\coth\mu\left(\alpha + \frac{in\pi}{2}\right). \tag{A.35}$$

One can show that the bootstrap equations imply

$$\sum_n (\delta_{kn} - (\delta_{k+1n} + \delta_{k-1n})s)(\delta_{nm} - \phi_{nm}) = \delta_{km}$$

where s is the inverse of the shift operator: $s^{-1}f(\alpha) = f(\alpha + \frac{i\pi}{2}) + f(\alpha - \frac{i\pi}{2})$.

Some formulas are easier to check in Fourier space. One can go to Fourier space using

$$\log[n] \sim \log\frac{-\sinh\mu(\theta + i\frac{n\pi}{2})}{\sinh\mu(\theta - i\frac{n\pi}{2})} = -i\int_{-\infty}^{\infty}\frac{dk}{k}\sin k\theta\frac{\sinh\frac{k\pi}{2\mu}(1-n\mu)}{\sinh\frac{k\pi}{2\mu}}. \tag{A.36}$$

In calculating the TBA equations the relation between massive-massive scattering and the massive-magnon scattering is also important. By inspecting the Fourier transforms we can see that

$$\phi_{00}(\theta) = \int_{-\infty}^{\infty} dk \frac{\sinh\frac{k\pi(1-\mu)}{2\mu}}{2\sinh\frac{k\pi}{2\mu}\cosh\frac{k\pi}{2}}\cos k\theta \tag{A.37}$$

where we removed the $\frac{1}{\sinh\mu(\theta - i\pi)}$ factor, since its inverse appears from the matrix part of the scattering. The operator s in Fourier space acts as multiplication with

$$s = \frac{1}{2\cosh\frac{k\pi}{2}} \tag{A.38}$$

we can thus see, that

$$\phi_{00} - s\star\phi_{10} = 0. \tag{A.39}$$

Let us investigate the shifted scatterings eq. (2.16). The corresponding $S_{0\bar{0}}$ can be obtained by multiplying $\tilde{U}(\theta)$ with $\cosh(\mu(\theta - i\pi))$ coming from the scattering matrix elements:

$$S_{0\bar{0}}(\theta) = \exp\left\{-i\int_0^{\infty}\frac{dk}{k}\frac{\sinh\frac{k\pi}{2}}{\sinh\frac{k\pi}{2\mu}\cosh\frac{k\pi}{2}}\sin k\theta\right\}. \tag{A.40}$$

The scattering between the massive node and the magnons will be also shifted

$$S_1(\alpha + i\beta) = \frac{\sinh\mu(\alpha + i\beta - \frac{i\pi}{2})}{\sinh\mu(\alpha + i\beta + \frac{i\pi}{2})}. \tag{A.41}$$

By choosing $\beta = \frac{\pi}{2\mu}$ we get

$$S_{10}(\alpha + i\beta) = \frac{\sinh[\mu(\alpha - \frac{i\pi}{2}) + \frac{i\pi}{2}]}{\sinh[\mu(\alpha + \frac{i\pi}{2}) + \frac{i\pi}{2}]} = \frac{\cosh\mu(\alpha - \frac{i\pi}{2})}{\cosh\mu(\alpha + \frac{i\pi}{2})} = -S_{p-10}(\alpha)^{-1} \tag{A.42}$$

JHEP11(2024)078

In calculating the kernels the relation is

$$\phi_{10}(\alpha + i\beta) = \phi_{1\bar{0}}(\alpha) = -\phi_{p-10}(\alpha). \tag{A.43}$$

One can also check that

$$\phi_{\bar{0}0} + \phi_{p-10} \star s = 0. \tag{A.44}$$

Thus all the kernel identities we used are satisfied.

A.3.2 Comments

Let us make a final comment about this approach. The Bethe Ansatz equations are basically the same as the XXZ Bethe ansatz equations. However not all solutions appear in the RSOS level. This means that some solutions have to be projected out. This was done in [34]. However this truncation does not seem to be compatible with the $\bar{n} = M + 1 - n$ relations.

A correct way of deriving the Bethe ansatz was based on the investigation of the distribution of zeroes of the transfer matrix fusion hierarchy in [35]. In this way the authors reproduced the massive and the interpolating massless TBA equations as the thermodynamic limit of an integrable lattice model. This ensures that the final TBA equations are indeed correct. We believe that the correct approach to obtain the same result from the TBA language would be to follow this analysis and analyze the zeros of the RSOS transfer matrix fusion hiearchy in the shifted inhomogenous case, instead of the solutions of the Bethe ansatz equations. This is, however, beyond the scope of this paper. We initiated a research into this direction.

Open Access. This article is distributed under the terms of the Creative Commons Attribution License (CC-BY4.0), which permits any use, distribution and reproduction in any medium, provided the original author(s) and source are credited.

JHEP11(2024)078

References

[1] A.B. Zamolodchikov, *Integrals of Motion and S Matrix of the (Scaled) T=T(c) Ising Model with Magnetic Field*, *Int. J. Mod. Phys. A* **4** (1989) 4235 [INSPIRE].

[2] A.B. Zamolodchikov, *Irreversibility of the Flux of the Renormalization Group in a 2D Field Theory*, *JETP Lett.* **43** (1986) 730 [INSPIRE].

[3] A.B. Zamolodchikov, *Thermodynamic Bethe Ansatz in Relativistic Models. Scaling Three State Potts and Lee-yang Models*, *Nucl. Phys. B* **342** (1990) 695 [INSPIRE].

[4] A.B. Zamolodchikov, *From tricritical Ising to critical Ising by thermodynamic Bethe ansatz*, *Nucl. Phys. B* **358** (1991) 524 [INSPIRE].

[5] A.B. Zamolodchikov, *TBA equations for integrable perturbed $SU(2)_k \times SU(2)_l/SU(2)_{k+l}$ coset models*, *Nucl. Phys. B* **366** (1991) 122 [INSPIRE].

[6] A.B. Zamolodchikov and A.B. Zamolodchikov, *Massless factorized scattering and sigma models with topological terms*, *Nucl. Phys. B* **379** (1992) 602 [INSPIRE].

[7] P. Fendley, H. Saleur and A.B. Zamolodchikov, *Massless flows, 2. The Exact S matrix approach*, *Int. J. Mod. Phys. A* **8** (1993) 5751 [hep-th/9304051] [INSPIRE].

[8] V.A. Fateev and A.B. Zamolodchikov, *Integrable perturbations of Z_N parafermion models and the $O(3)$ sigma model*, *Phys. Lett. B* **271** (1991) 91 [INSPIRE].

[9] P. Dorey, C. Dunning and R. Tateo, *New families of flows between two-dimensional conformal field theories*, *Nucl. Phys. B* **578** (2000) 699 [hep-th/0001185] [INSPIRE].

[10] C. Ahn, C. Kim, C. Rim and A.B. Zamolodchikov, *RG flows from superLiouville theory to critical Ising model*, *Phys. Lett. B* **541** (2002) 194 [hep-th/0206210] [INSPIRE].

[11] C. Ahn and A. LeClair, *On the classification of UV completions of integrable $T\overline{T}$ deformations of CFT*, *JHEP* **08** (2022) 179 [arXiv:2205.10905] [INSPIRE].

[12] F.A. Smirnov and A.B. Zamolodchikov, *On space of integrable quantum field theories*, *Nucl. Phys. B* **915** (2017) 363 [arXiv:1608.05499] [INSPIRE].

[13] A. Cavaglià, S. Negro, I.M. Szécsényi and R. Tateo, *$T\bar{T}$-deformed 2D Quantum Field Theories*, *JHEP* **10** (2016) 112 [arXiv:1608.05534] [INSPIRE].

[14] D. Bernard and A. Leclair, *Residual Quantum Symmetries of the Restricted Sine-Gordon Theories*, *Nucl. Phys. B* **340** (1990) 721 [INSPIRE].

[15] C. Copetti, L. Cordova and S. Komatsu, *Noninvertible Symmetries, Anomalies, and Scattering Amplitudes*, *Phys. Rev. Lett.* **133** (2024) 181601 [arXiv:2403.04835] [INSPIRE].

[16] A.B. Zamolodchikov, *Thermodynamic Bethe ansatz for RSOS scattering theories*, *Nucl. Phys. B* **358** (1991) 497 [INSPIRE].

[17] A.B. Zamolodchikov, *Mass scale in the sine-Gordon model and its reductions*, *Int. J. Mod. Phys. A* **10** (1995) 1125 [INSPIRE].

[18] A.B. Zamolodchikov, *Resonance factorized scattering and roaming trajectories*, *J. Phys. A* **39** (2006) 12847 [INSPIRE].

[19] A.B. Zamolodchikov and A.B. Zamolodchikov, *Structure constants and conformal bootstrap in Liouville field theory*, *Nucl. Phys. B* **477** (1996) 577 [hep-th/9506136] [INSPIRE].

[20] A.B. Zamolodchikov and V.A. Fateev, *Nonlocal (parafermion) currents in two-dimensional conformal quantum field theory and self-dual critical points in Z_n-symmetric statistical systems*, *Sov. Phys. JETP* **62** (1985) 215 [INSPIRE].

[21] C. Ahn, D. Bernard and A. LeClair, *Fractional Supersymmetries in Perturbed Coset Cfts and Integrable Soliton Theory*, *Nucl. Phys. B* **346** (1990) 409 [INSPIRE].

[22] C. Destri and H.J. de Vega, *New exact results in affine Toda field theories: Free energy and wave function renormalizations*, *Nucl. Phys. B* **358** (1991) 251 [INSPIRE].

[23] R.H. Poghossian, *Structure constants in the N=1 superLiouville field theory*, *Nucl. Phys. B* **496** (1997) 451 [hep-th/9607120] [INSPIRE].

[24] R.C. Rashkov and M. Stanishkov, *Three point correlation functions in $N = 1$ superLiouville theory*, *Phys. Lett. B* **380** (1996) 49 [hep-th/9602148] [INSPIRE].

[25] R. Shankar and E. Witten, *The S Matrix of the Supersymmetric Nonlinear σ Model*, *Phys. Rev. D* **17** (1978) 2134 [INSPIRE].

[26] C.-R. Ahn, *Complete S matrices of supersymmetric Sine-Gordon theory and perturbed superconformal minimal model*, *Nucl. Phys. B* **354** (1991) 57 [INSPIRE].

[27] P. Baseilhac and V.A. Fateev, *Expectation values of local fields for a two-parameter family of integrable models and related perturbed conformal field theories*, *Nucl. Phys. B* **532** (1998) 567 [hep-th/9906010] [INSPIRE].

JHEP11(2024)078

[28] P. Dorey and F. Ravanini, *Generalizing the staircase models*, *Nucl. Phys. B* **406** (1993) 708 [hep-th/9211115] [INSPIRE].

[29] P.E. Dorey and F. Ravanini, *Staircase models from affine Toda field theory*, *Int. J. Mod. Phys. A* **8** (1993) 873 [hep-th/9206052] [INSPIRE].

[30] S. Frolov and A. Sfondrini, *Massless S matrices for AdS3/CFT2*, *JHEP* **04** (2022) 067 [arXiv:2112.08895] [INSPIRE].

[31] C. Dunning, *Massless flows between minimal W models*, *Phys. Lett. B* **537** (2002) 297 [hep-th/0204090] [INSPIRE].

[32] C.-M. Chang et al., *Topological Defect Lines and Renormalization Group Flows in Two Dimensions*, *JHEP* **01** (2019) 026 [arXiv:1802.04445] [INSPIRE].

[33] R.A. Janik and T. Lukowski, *From nesting to dressing*, *Phys. Rev. D* **78** (2008) 066018 [arXiv:0804.4295] [INSPIRE].

[34] V.V. Bazhanov and N.Y. Reshetikhin, *Critical Rsos Models and Conformal Field Theory*, *Int. J. Mod. Phys. A* **4** (1989) 115 [INSPIRE].

[35] P.A. Pearce and B. Nienhuis, *Scaling limit of RSOS lattice models and TBA equations*, *Nucl. Phys. B* **519** (1998) 579 [hep-th/9711185] [INSPIRE].

JHEP11(2024)078